Electrophysiological characterization and molecular identification of the *Phoneutria nigriventer* peptide toxin PnTx2-6[1]

Alessandra Matavel[a], Jader S. Cruz[a], Claudia L. Penaforte[a], Demétrius A.M. Araújo[b], Evanguedes Kalapothakis[c], Vânia F. Prado[a], Carlos R. Diniz[a,d], Marta N. Cordeiro[d], Paulo S.L. Beirão[a,*]

[a] *Department of Biochemistry and Immunology, Instituto de Ciências Biológicas, Universidade Federal de Minas Gerais, Caixa Postal 486, 30161-970 Belo Horizonte, MG, Brazil*
[b] *Department of Molecular Biology, Universidade Federal da Paraíba, João Pessoa, PB, Brazil*
[c] *Department of Pharmacology, Instituto de Ciências Biológicas, Universidade Federal de Minas Gerais, Belo Horizonte, MG, Brazil*
[d] *Fundação Ezequiel Dias, Belo Horizonte, MG, Brazil*

Received 29 April 2002; revised 14 June 2002; accepted 17 June 2002

First published online 26 June 2002

Edited by Maurice Montal

Abstract A cDNA with 403 nucleotides encoding the precursor of the toxin PnTx2-6 was cloned and sequenced. Subsequent analysis revealed that the precursor begins with a signal peptide and a glutamate-rich propeptide. The succeeding peptide confirmed the reported sequence of PnTx2-6. The purified toxin exerted complex effects on Na^+ current of frog skeletal muscle. There was a marked decrease of the inactivation kinetics, and a shift to hyperpolarizing potentials of both the Na^+ conductance and the steady-state inactivation voltage dependences, along with a reduction of the current amplitude. The concentration dependence of the modified current suggests a K_D of 0.8 μM for the toxin–channel complex. © 2002 Published by Elsevier Science B.V. on behalf of the Federation of European Biochemical Societies.

Key words: PnTx2-6; Spider toxin; Peptide toxin; Neurotoxin; Sodium channel; *Phoneutria nigriventer*

1. Introduction

An important feature of normal Na^+ channel function is fast inactivation. It plays a key role in keeping short the duration of nerve and skeletal muscle action potentials and is caused by the movement of the intracellular IIIS4-IVS1 linker [1].

The vital role of fast inactivation is unveiled by the existence of several types of toxins that inhibit it, thus causing excitatory syndrome that leads to paralysis and death. Toxins with different structures, and even different chemical natures, may exert similar effects. Interestingly, many of these toxins are polypeptides that act on the outside of the membrane, and affect the movement of the intracellular IIIS4-IVS1 linker. Evidence shows that this may occur by altering the coupling of inactivation to activation [2].

Spider venoms have been used as a potential source of new compounds with specific pharmacological properties. The *Phoneutria nigriventer* venom is a rich source of bioactive peptides [3,4]. Recently a cDNA library of the *P. nigriventer* venom gland was described and used to identify peptides expressed by the gland cells [5].

Araújo et al. [6] showed that the toxic effect of fraction PhTx2, which causes the predominant effects of *P. nigriventer* venom, could be attributed to an inhibition of Na^+ channel fast inactivation. One of the PhTx2 components is the *P. nigriventer* toxin Tx2-6 [7], which we will refer to as PnTx2-6. In the present study we report the full cDNA sequence and the electrophysiological characterization of PnTx2-6 effects on Na^+ currents, showing that: (1) the time constant for fast inactivation is greatly slowed; (2) the voltage dependence of the Na^+ conductance and of the steady-state inactivation is shifted to the hyperpolarized direction; (3) the peak current is decreased at almost all potentials. We also propose that PnTx2-6 is synthesized as a prepropeptide, with a signal peptide with 17 residues and a glutamate-rich intervening propeptide with 17 amino acids. The reported sequence of the 48 amino acid mature toxin was confirmed, including the presence of 10 cysteines.

2. Materials and methods

2.1. Electrophysiological assay

Sodium currents were recorded from frog (*Rana catesbeiana*) semitendinous muscle using the loose patch clamp technique, as previously described [6]. Pipettes (tip diameters = 14–29 μm) were filled with a modified Ringer's solution (in mM: NaCl 115, KCl 2.5, $CaCl_2$ 1.8, 4-aminopyridine 10 and HEPES 5.0, pH 7.2), with 0.1% bovine serum albumin. PnTx2-6 was added to the pipette solution, as appropriate. The pipette resistances (R_p) and loose seal resistances (R_s) ranged from 0.24 to 0.62 MΩ and 1.20 to 2.65 MΩ, respectively. The loose patch clamp amplifier (Dagan 8900, with probe model 8970) contains an impedance bridge that compensates for R_p and R_s, thus keeping the voltage at the pipette tip under control [8]. To avoid 'rim currents', the fibers were maintained depolarized in a bath solution with 27 mM K^+ (in mM: sodium acetate 88, potassium acetate 16, KCl 11, calcium propionate 1.8 and HEPES 5.0, pH 7.2, adjusted with NaOH), which depolarizes the fibers to −43 mV, thereby inactivating Na^+ channels [9]. By hyperpolarizing the membrane patch to −93 mV (holding potential) for at least 10 min, the fast and slow inactivation of the sodium channels under voltage control were selectively removed [6,10]. The bath temperature was kept at 10–12°C, to slow down Na^+ current kinetics.

Ionic currents were filtered (10 kHz low-pass filter) and sampled at 30 kHz with a 12 bit analog-to-digital converter (Engenharia Eletro-

*Corresponding author. Fax: (55)-31-441 5963.
E-mail address: pslb@ufmg.br (P.S.L. Beirão).

[1] Nucleotide sequence data reported are available in the GenBank database under accession number AY054746.

0014-5793/02/$22.00 © 2002 Published by Elsevier Science B.V. on behalf of the Federation of European Biochemical Societies.
PII: S0014-5793(02)02988-5

Eletrônica, São Paulo, Brazil). Data acquisition and analysis were carried out with a suite of programs written in Pascal by P.S.L. Beirão. The P/4 protocol was used to subtract linear leakage and capacitative currents.

2.2. Screening and identification of PnTx2-6

Standard recombinant DNA techniques were carried out as described elsewhere [11]. Using the cDNA library and the methodology described previously [5], the cDNA encoding PnTx2-6 was obtained. The clone was sequenced on both strands using the chain termination method [12] with an automated ALF DNA sequencer (Pharmacia). Nucleic acid sequences were analyzed and compared using both the BLAST-X algorithm [13] and PC/GENE software system.

Northern blots were carried out as described previously [5], using total RNA purified from the venom gland and from the spider body (without the glands) [14].

2.3. Toxin purification

The venom was fractionated by sequential molecular filtration and reverse phase chromatography to obtain the neurotoxic fraction PhTx2, which was chromatographed by reverse phase HPLC on analytical Vydac C18, using an extended linear gradient of acetonitrile 0.1% (v/v) in aqueous solution of trifluoroacetic acid. PnTx2-6 eluted in a homogeneous peak at 37% acetonitrile (for details see [7]).

2.4. Statistics

The results are expressed as means ± S.E.M. Student's *t*-test was used to calculate the statistical significance of differences between means, considering $P < 0.05$ an indication of statistical significance.

3. Results

3.1. P. nigriventer toxin PnTx2-6 inhibits inactivation of sodium currents

Control and toxin-treated Na^+ currents are shown in Fig. 1A. The marked slowing of inactivation can be better appreciated in Fig. 1B, where two representative records are superimposed, which also shows that the time course of Na^+ current activation is not altered.

Fig. 1C shows a significant decrease of the peak inward current density at all potentials, except those lower than −40 mV. Under control conditions, inward currents activated in response to depolarizing test pulses at about −45 mV, and reached a maximum at −13 mV. A close examination of this figure indicates that PnTx2-6 shifted the activation threshold to hyperpolarizing potentials, whereas the peak inward Na^+ current, although decreased (45% at −13 mV), was not shifted.

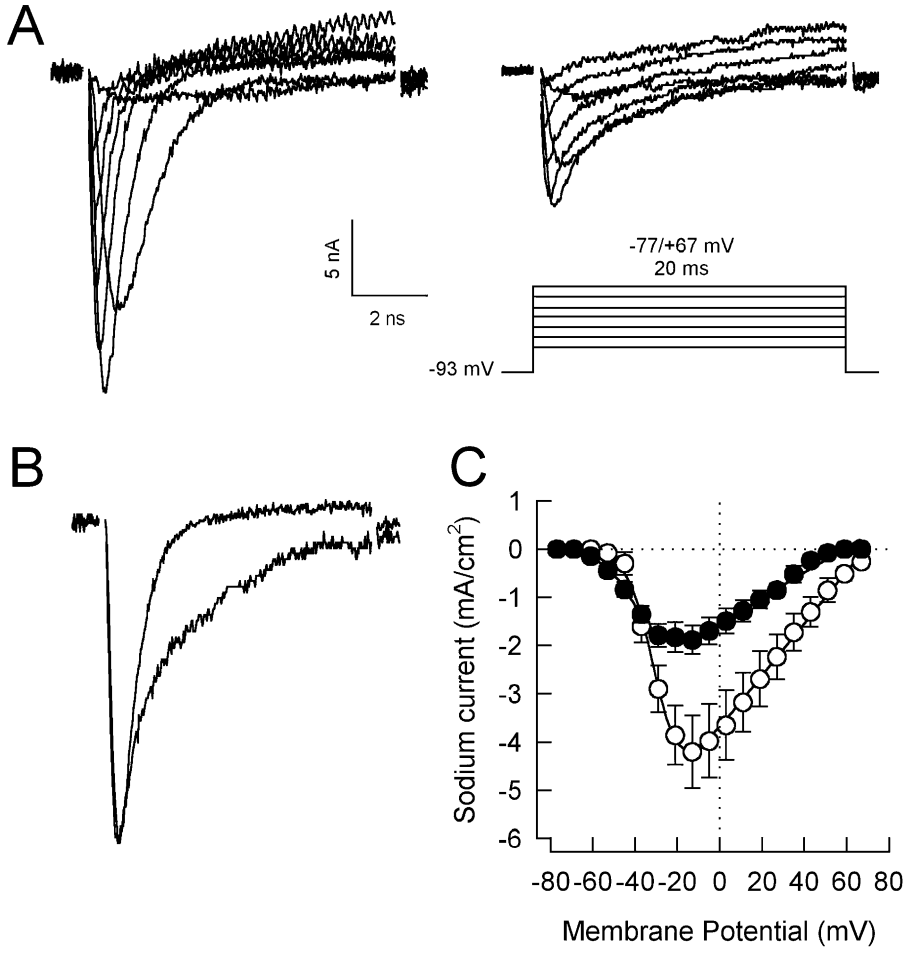

Fig. 1. Effects of PnTx2-6 on Na^+ currents. A: Representative records of Na^+ currents in response to step depolarizations, as shown in the inset. Left panel: control. Right panel: in the presence of 1 μM PnTx2-6. B: For comparison, control and experimental Na^+ currents elicited at −13 mV were scaled and superimposed. C: Na^+ current density × voltage in control (open circles, $n = 12$) and in 1 μM PnTx2-6 (closed circles, $n = 7$). The graph was fitted by the equation $I_{Na} = g_{Na(max)} * (V_m - V_r)/\{1+\exp[(V_g - V_m)/K_g]\}$, where $g_{Na(max)}$ is the maximal conductance, V_m is the membrane potential, V_r is the reversal potential, V_g is the potential for half-maximal conductance, K_g is the slope factor. The parameters of control and in the presence of PnTx2-6 are, respectively: $g_{Na(max)} = 54.5 \pm 9.4$ and 26.5 ± 2.9 mS/cm^2; $V_r = 67.3 \pm 1.7$ and 57.8 ± 1.3 mV; $V_g = -31.5 \pm 1.6$ and -39.2 ± 2.6 mV and $K_g = 5.5 \pm 0.1$ and 7.28 ± 0.3.

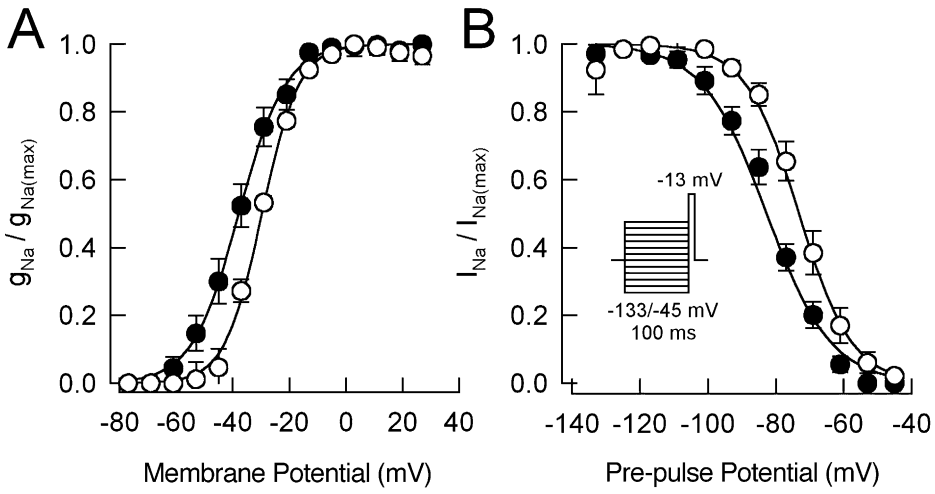

Fig. 2. PnTx2-6 alters the voltage dependence of the Na^+ conductance and of the steady-state inactivation. A: Normalized peak conductance is plotted as a function of membrane voltage. Control (open circles, $n=12$) and experimental (1 μM PnTx2-6, closed circles, $n=7$) points were fitted with the Boltzmann equation: $g_{Na}/g_{Na(max)} = \{1+\exp[(V_g-V_m)/K_g]\}^{-1}$. Best fit parameters for control and experimental data were, respectively: $V_g = -30.3 \pm 1.6$ and -38.7 ± 2.9 mV; $K_g = 5.8 \pm 0.2$ and 7.7 ± 0.4. B: Normalized peak inward current is plotted as a function of the 100 ms prepulse membrane potential. The experimental protocol is shown in the inset. Control (open circles, $n=12$) and experimental (1 μM PnTx2-6, closed circles, $n=7$) points were fitted with the Boltzmann equation: $I_{Na}/I_{Na(max)} = \{1+\exp[V_p-V_h)/K_h]\}^{-1}$, where V_p is the prepulse membrane potential, V_h is the potential for half-maximal steady-state inactivation, and K_h is the slope factor for steady-state inactivation. Best fit parameters for control and experimental data were, respectively: $V_h = -72.8 \pm 2.1$ and -82.8 ± 2.0 mV; $K_h = 6.7 \pm 0.2$ and 9.0 ± 0.9.

3.2. *The Na^+ conductance and the steady-state inactivation voltage dependences are changed by PnTx2-6*

The observed hyperpolarizing shift (Fig. 1C) suggests that PnTx2-6 affects the voltage dependence of the Na^+ conductance (g_{Na}). Fig. 2A shows the normalized Na^+ conductance plotted as a function of membrane potential in the absence and in the presence of 1 μM PnTx2-6. There was a small (−8.5 mV) but significant shift of its voltage dependence, which also became less steep, as indicated by the increase of the slope factor K_g.

The steady-state inactivation in the presence of 1 μM PnTx2-6 was studied using the protocol shown in Fig. 2B (inset). PnTx2-6 caused a significant (10.0 mV) hyperpolarizing shift of the voltage where 50% of the channels were inactivated. These results are similar to those described for the PhTx2 fraction [6] leading to the conclusion that PnTx2-6 can account for its major toxic effects.

3.3. *Kinetic analysis of PnTx2-6 effect*

The striking slowing of the inactivation rate noticed in Fig. 1A was further investigated by studying the time course of inactivation at different membrane potentials. The inactivation of control Na^+ currents follows a monoexponential decay. It becomes biexponential in the presence of PnTx2-6, having a fast component with a time constant equal to control at all potentials, and a slower component, with a time constant one order of magnitude larger (Fig. 3A,B). The slow time course induced by PnTx2-6 showed a conspicuous dispersion of the data, and no voltage dependence could be assigned.

We attribute the biexponential behavior of inactivation to the presence of free and toxin-bound channels, generating the fast and slow components, respectively, because the fast component was not different from control, and the slow component was never found in control. In support to this interpretation we observed that the proportion of the slow component increases with the concentration of PnTx2-6 (Fig. 3C). The continuous line in the figure represents the best fit of a quadratic hyperbola equation to the experimental data, assuming a one-to-one binding scheme. The calculated $E_{(max)}$ suggests that PnTx2-6 may be unable to modify completely the Na^+ channels.

The recovery from inactivation was also investigated, and Fig. 3D shows that it is decreased by PnTx2-6.

3.4. *Molecular biology of PnTx2-6*

One hundred and eighty-five clones, obtained from the venom glands of 15 spiders whose venom had been extracted 2 days before, were analyzed and the sequences obtained compared to those contained in the GenBank database. Approximately 10% of the deduced peptide sequences showed homology to previously known toxins, including one clone that contained a nucleotide sequence that encoded the previously reported sequence of PnTx2-6 [7]. Sequence analysis showed that this cDNA (with 403 bp) contained, at its ends, a 5′ untranslated region composed of 94 bp and a short 3′ untranslated region showing the consensus site for the polyadenylation signal (AATAAA) upstream to the poly(A) tract.

Total RNA from *P. nigriventer* body and venom gland were examined by Northern blot using the cDNA isolated from the clone PnTx2-6. It showed a single band on the gland RNA of approximately 400 bp (not shown), supporting the idea that we have isolate a full length cDNA clone of this toxin. The open reading frame of the isolated cDNA encode a peptide (82 amino acid residues) that was longer than the mature toxin (48 amino acid residues). As shown in Fig. 4, the extra 34 amino acid residues form a sequence that precedes the toxin peptide. The first 17 amino acid sequence is hydrophobic and shows all characteristics of a typical signal peptide [15], including a consensus cleavage point for a signal peptidase. The intervening propeptide, composed of 17 amino acid

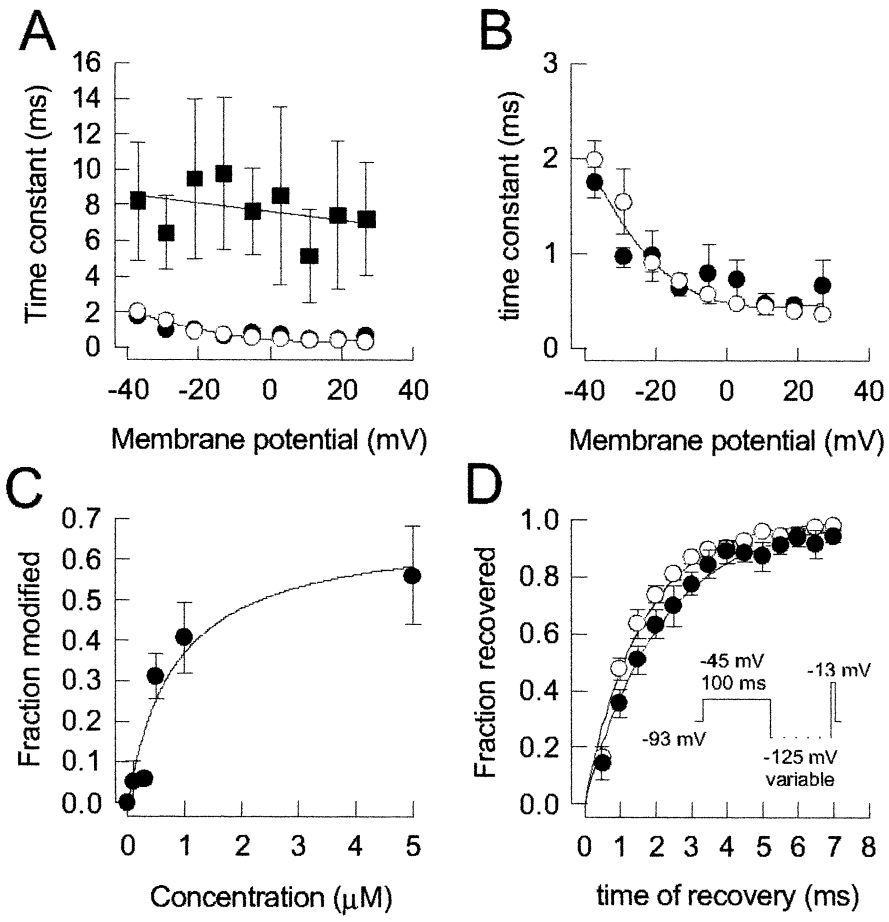

Fig. 3. Effects of PnTx2-6 on the kinetics of inactivation. A: Time constant of inactivation as a function of potential in control (open circles) and experimental (1 μM PnTx2-6, closed circles, fast component; closed squares, slow component). The time constants were obtained by fitting each current decay with the equation: $f = a\exp(-t/\tau_{fast}) + b\exp(-t/\tau_{slow})$, where t is the time after the current peak and $b = 0$ for control records. B: The control time constant (open circles) and the fast component in the presence of 1 μM PnTx2-6 are replotted on an expanded scale. C: The proportion of the slow component [$b/(a+b)$] obtained by the equation shown in A is plotted at different concentrations (c) of PnTx2-6. The curve was drawn with the quadratic hyperbola equation: $f = E_{(max)}c/(K_{0.5}+c)$, where the best fit was obtained with $K_{0.5} = 0.81$ μM and $E_{(max)} = 0.68$. D: The fraction of the sodium current recovered at −125 mV, after a 100 ms pulse to −45 mV that fully inactivated the current, is plotted against the time allowed for recovery. The protocol is shown in the insert. Data are fitted with the equation: $f = 1-\exp(-t/\tau_r)$, and the time constants of recovery (τ_r) were 1.60 ± 0.14 ms and 2.14 ± 0.23 ms for control and experimental, respectively.

residues, is rich in glutamate residues and contained an arginine at the C-terminus. We propose that PnTx2-6 is synthesized and processed as a prepropeptide toxin, as has been shown for the *P. nigriventer* toxin that act on calcium channels [5].

4. Discussion

In this article we describe the primary structure, processing and effects of *P. nigriventer* PnTx2-6 toxin. The cDNA sequence confirmed the reported structure of the mature toxin

```
                  ***
tcggcacgagatcaga ATG AAA GTT GCA ATC CTC TTC CTC TCT ATT TTG GTG CTT GCT GTT GCA AGT
                  M   K   V   A   I   L   F   L   S   I   L   V   L   A   V   A   S

GAA TCC ATT GAA GAA TCC CGT GAT GAT TTT GCT GTA GAA GAA TTG GGG AGA
 E   S   I   E   E   S   R   D   D   F   A   V   E   E   L   G   R

GCC ACA TGC GCT GGC CAA GAC CAG CCC TGC AAA GAA ACT TGC GAC TGC TGT GGA GAG AGA GGA GAA TGT GTT
 A   T   C   A   G   Q   D   Q   P   C   K   E   T   C   D   C   C   G   E   R   G   E   C   V

TGC GGA GGA CCT TGC ATT TGC AGG CAA GGC TAC TTT TGG ATA GCA TGG TAT AAA CTT GCT AAC TGT AAA AAA
 C   G   G   P   C   I   C   R   Q   G   Y   F   W   I   A   W   Y   K   L   A   N   C   K   K

***
tga tatggatttatgtataccacgatataataaatatattgcatttgaaaaaaaaaaaaaa    323
```

Fig. 4. cDNA and deduced amino acid sequence of PnTx2-6. The coding region is shown in upper case, with the 5′ and 3′ untranslated regions in lower case. Initiation (ATG) and stop (TGA) codons are highlighted with asterisks. The hydrophobic region (signal peptide) is in italics, followed by the underlined hydrophilic region (propeptide). The mature toxin is in bold characters.

and showed that it is synthesized as a preprotoxin. The sequence of the toxin was found to have no significant identity with sequences of other species found in BLAST databases. However, the three-dimensional structures of a number of peptides, which specifically act on different ion channels, have been shown to contain similar structural motifs, despite the lack of sequence homology [16,17]. The similarity of effects in comparison with the difference in structure may provide invaluable information of the structural determinants of each activity.

The presence of a short glutamate-rich propeptide has been previously described in spider toxin precursors including the ω-agatoxin IA from *Agelenopsis aperta* [18] and the Tx1 from *P. nigriventer* [19], with 35% and 27% sequence identity with PnTx2-6, respectively. However, its function is still not clear. Possible roles have been suggested, including targeting to enzymes required for post-translational modifications; directing intracellular trafficking to secretory granules; or a role in folding, by enhancing the solubility of the nascent chain and promoting interactions with other cellular factors [20].

PnTx2-6 can be classified as a peptide toxin that alters voltage-dependent gating of sodium channels. Its activity is similar to 'site 3' toxins, causing a marked slowing of inactivation [2], without changing the time to reach the peak of the current, at all potentials (not shown). In contrast, it also shifts the voltage dependence of the Na^+ conductance to negative potentials and decreases the peak inward current. It has been demonstrated that procedures that selectively slow the transition from open to inactivated states may bring on a negative shift of the conductance voltage dependence, and an increase (and not a decrease) of the peak current [21]. This is the typical effect of α-scorpion toxins. On the other hand, β-scorpion toxins produce a negative shift of the Na^+ conductance and decrease the peak current, without affecting the rate of inactivation. Our results suggest a complex effect of PnTx2-6 that does not conform to either a typical α- or β-type activity. Similar effects were reported for robustoxin and versutoxin, which have a pronounced effect on sodium channel inactivation, and simultaneously decrease the peak inward current and shift both the Na^+ conductance and the steady-state inactivation voltage dependences to negative potentials. In contrast, 1 s depolarizing (−40 mV) prepulses failed to fully inactivate a significant fraction of Na^+ channels [22], not seen with PnTx2-6 (Fig. 2B). It was also reported that robustoxin produces a significant increase in the kinetics of Na^+ channel recovery from inactivation, differently from PnTx2-6 (Fig. 3D).

In summary, the main action of PnTx2-6 is to slow down sodium channel fast inactivation. This effect is followed by significant changes in the voltage dependence of both the Na^+ conductance and the steady-state inactivation, which suggests a mechanism somehow different from the classical α-toxins. Further binding studies are required to identify if PnTx2-6 competes with α-scorpion toxin binding. Nevertheless, the present study brings up the indication that PnTx2-6 can modify Na^+ channel inactivation and paves the way for further investigation exploring the existence of a macrosite, where different toxins with diverse structures may elicit similar pharmacological responses.

Acknowledgements: This project was supported by CNPq, FAPEMIG and PADCT.

References

[1] Catterall, W.A. (2000) Neuron 26, 13–25.
[2] Cèstele, S. and Catterall, W.A. (2000) Biochemie 82, 883–892.
[3] Cordeiro, M.N., Richardson, M., Gilroy, J., Figueiredo, S.G., Beirão, P.S.L. and Diniz, C.R. (1995) J. Toxicol. Toxin Rev. 14, 309–326.
[4] Leão, R.M., Cruz, J.S., Diniz, C.R., Cordeiro, M.N. and Beirão, P.S.L. (2000) Neuropharmacology 39, 1756–1767.
[5] Kalapothakis, E., Penaforte, C.L., Beirão, P.S.L., Romano-Silva, M.A., Cruz, J.S., Prado, M.A.M., Guimarães, P.E.M., Gomez, M.V. and Prado, V.F. (1998) Toxicon 36, 1843–1850.
[6] Araújo, D.A.M., Cordeiro, M.N., Diniz, C.R. and Beirão, P.S.L. (1993) Naunyn-Schmiedeberg's Arch. Pharmacol. 347, 205–208.
[7] Cordeiro, M.N., Diniz, C.R., Valentim, A.C., Von Eickstedt, V.R.D., Gilroy, J. and Richardson, M. (1992) FEBS Lett. 310, 153–156.
[8] Stühmer, W., Roberts, W.M. and Almers, W. (1983) in: Single Channels Recording (Sakmann, B. and Neher, E., Eds.), Vol. 1, pp. 123–132, Plenum Press, New York.
[9] Almers, W., Stanfield, P.R. and Stühmer, W. (1983) J. Physiol. 336, 261–284.
[10] Matavel, A.C.S., Ferreira-Alves, D.L., Beirão, P.S.L. and Cruz, J.S. (1998) Eur. J. Pharmacol. 348, 167–173.
[11] Sambrook, J., Fritsch, E.F. and Maniatis, T. (1989) Molecular Cloning: A Laboratory Manual, 2nd edn., Cold Spring Harbor Laboratory Press, Cold Spring Harbor, NY.
[12] Sanger, F., Nicklen, F.S. and Coulson, A.R. (1977) Proc. Natl. Acad. Sci. USA 74, 5463–5467.
[13] Altschul, S.F., Gish, W., Miller, W., Myers, E.W. and Lipman, D. (1990) Proc. Natl. Acad. Sci. USA 90, 4338–4344.
[14] Perlman, D. and Halvorson, H.O. (1983) J. Mol. Biol. 167, 391–409.
[15] Chomczynski, P. and Sacchi, N. (1987) Anal. Biochem. 162, 156–159.
[16] Omecinsky, D.O., Holub, K.E., Adams, M.E. and Reily, M.D. (1996) Biochemistry 35, 2836–2844.
[17] Kim, J.I., Konishi, S., Iwai, H., Kohno, T., Gouda, H., Shimada, I., Sato, K. and Arata, Y. (1995) J. Mol. Biol. 250, 659–671.
[18] Santos, A.D., Imperial, J.S., Chaudhary, T., Beavis, R.C., Chait, B.T., Hunsperger, J.P., Oliveira, B.M., Adams, M.E. and Hillyard, D.R. (1992) J. Biol. Chem. 267, 20701–20705.
[19] Diniz, M.R.V., Paine, M.J.I., Diniz, C.R., Theakston, R.D.G. and Crampton, J.M. (1993) J. Biol. Chem. 268, 15340–15342.
[20] Price-Carter, M., Gray, W.R. and Goldenberg, D.P. (1996) Biochemistry 35, 15547–15557.
[21] Gonoi, T. and Hille, B. (1987) J. Gen. Physiol. 89, 253–274.
[22] Nicholson, G.M., Walsh, R., Little, M. and Tyler, M.I. (1998) Pflügers Arch. Eur. J. Physiol. 436, 117–126.